Using Electrochemical Impedance Spectroscopy to Characterize Vertically-Aligned Carbon Nanotube Forest Porosimetry

by

Yuan Lu

Submitted to the Department of Materials Science and Engineering in partial fulfillment of the requirements for the degree of

Bachelor of Science in Materials Science and Engineering

at the

Massachusetts Institute of Technology

June 2015

Signature of Author: Signature redacted

Yuan Lu
Department of Materials Science and Engineering
May 8, 2015

Certified by: Signature redacted

Evelyn N. Wang
Associate Professor of Mechanical Engineering
Thesis Supervisor

Certified by: Signature redacted

Carl V. Thompson
Professor of Materials Science and Engineering
Thesis Reader

Accepted by: Signature redacted

Geoffrey Beach
Chairman, Department Committee on Undergraduate Theses

Using Electrochemical Impedance Spectroscopy to Characterize Vertically-Aligned Carbon Nanotube Forest Porosimetry

by

Yuan Lu

Submitted to the Department of Materials Science and Engineering
in June 2015, in partial fulfillment of the requirements for the degree of
Bachelor of Science in Materials Science and Engineering

Abstract

Carbon nanotubes have generated much research interest and potential applications due to their unique properties such as their high tensile strength, high thermal conductivity, and unique semiconductor properties. Vertically-aligned carbon nanotubes (VA-CNTs) have been used in applications for electrochemical systems in energy storage systems and desalination systems. Typical methods of characterizing the morphology and composition of CNTs are limited in providing information on the packing density of CNTs, and therefore, an effective method for *in situ* characterization of VA-CNT electrodes is needed. This method explores the use of impedance spectroscopy and other electrochemical methods to characterize VA-CNTs *in situ*. VA-CNTs forests were grown via chemical vapor densification on pre-oxidized silicon wafers, mechanically densified to achieve varying volume fractions (1%, 2%, 5%, and 10%), and tested in a three-electrode electrochemical cell. Electrochemical techniques (cyclic voltammetry, impedance spectroscopy, and potentiostatic techniques) were used to measure the performance of the VA-CNTs in 1 M and 500 mM electrolyte solutions. Optimization of the experimental setup design and data collection methods yielded data that resulted in the expected cyclic voltammetry response and impedance behavior of porous electrodes. A transmission line model-pore size distribution (TLM-PSD) model was applied to the data collected in order to predict and model porosimetry characteristics. Porous behavior was observed in the VA-CNT electrodes of all volume fractions tested, and the impedance spectra showed that the volume fraction affected the overall impedance but not the characteristic shape of the spectra. Comparison between the impedance data collected in 1 M NaCl and 500 mM NaCl showed the expected corresponding inverse correlation with solution conductivity. Parameters that describe the VA-CNT electrode porosity were calculated and predicted using electrochemical data and the TLM-PSD model. The porous volume V_{tot} and total ionic conductance Y_p values calculated using the model applied to the impedance spectroscopy data showed trends as expected for the different volume fractions of VA-CNT. The results show that electrochemical impedance spectroscopy can be used to characterize certain physical characteristics of the VA-CNT electrodes and further development of the model can yield insights into the porous geometry of VA-CNT forests.

Acknowledgments

First and most important of all, I would like to thank Heena Mutha for everything. I am grateful for all of Heena's mentorship, guidance, and help from the very beginning to the end of this project. She has been incredibly supportive and an awesome person to work with, and this all would not have been possible without her.

I also would like to thank Professor Evelyn N. Wang and Professor Carl V. Thompson for their supervision in the thesis writing process. I would like to thank Professor Gang Chen for allowing us to run experiments on his lab's potentiostat and Professor Brian Wardle for letting me use his lab space, equipment, and instruments to carry out my project. In addition, I would like to thank Patrick Boisvert for his training and help with the scanning electron microscope in the CMSE facilities.

Lastly, I would like to thank all my friends who have been pillars of support throughout this thesis writing process.

Contents

List of Figures

List of Tables

Chapter 1. Introduction

Carbon nanotubes (CNTs) have a wide range of promising properties including high tensile strength, high electrical and thermal conductivity, and field emission capabilities [1, 2]. These desirable material properties of CNTs have generated diverse research areas investigating the role of CNT morphology for various applications ranging from high-strength composites to energy storage and conversion devices [1]. CNTs have been used in capacitor electrodes in electrochemical systems, such as those in energy storage systems [2] or desalination systems [3]. Vertically-aligned carbon nanotube (VA-CNT) forests can provide the benefits of CNT properties, along with alignment of electrodes leading to faster rates of charge and discharge. VA-CNT electrode performance as a capacitor or in a desalination cell relies on the capacitance of the CNT electrode, and previous research has shown that increased volume fraction of CNTs can yield higher volumetric capacitance [4]. In order to characterize the surface area and porous characteristics, typical carbon electrode materials methods such as Brannauer-Emmett-Teller (BET) analysis [5], where nitrogen or other gas is absorbed onto the material to generate direct measurements, are conducted. Other techniques such as Raman spectroscopy and microscopy imaging are also used to characterize CNTs and estimate the corresponding geometry, but many of these techniques also either destroy the sample or alter the sample's properties [6]. Thus, a direct method for *in situ* characterization of VA-CNT forest geometry is needed.

Electrochemical impedance spectroscopy techniques have been applied previously for *in situ* characterization modelling of porous electrode catalysts [8]. The research presented in this paper investigates a method of *in situ* porosimetry aspects of VA-CNT electrodes in electrolyte solution via electrochemical impedance spectroscopy. VA-CNT forests are modeled as cylindrical porous electrodes via the transmission line model with porous distribution (TLM-

PSD) to fit the impedance spectra. VA-CNT forests are grown via chemical vapor deposition and mechanically densified to produce varying volume fractions. The VA-CNT forests are placed in an electrochemical setup as the working electrodes and electrochemical techniques are used to examine and model the changing volume fractions. Using the electrochemical data collected, the parameters characterizing the porosity of CNT carpets are calculated and the changes in varying volume fractions are analyzed. This research will show the potential of using electrochemical techniques to characterize VA-CNT electrodes locally in electrochemical systems.

Chapter 2. Theory and Background

Knowledge of carbon nanotubes, porous electrodes, and electrochemical impedance methods were utilized to carry out this research effort. This section presents information on these topics and related sub-topics to build a background on the theory behind the research.

2.1. Carbon Nanotubes

CNTs were first identified in 1991 by Sumio Iijima via high resolution transmission electron microscopy (TEM) [9]. Since their discovery, carbon nanotubes have been of much interest within physics, chemistry, and materials science [6]. Numerous research and development on the structure, properties, and potential applications of CNTs have been made in the past few decades. Their unique, diverse range of properties give them high potential to be breakthroughs for many applications and products. This section will give a brief overview on the structure and properties, applications, and characterization methods of CNTs.

2.1.1. Structure and Properties

Carbon nanotubes are graphene sheets rolled into tubes and can exist as single walled carbon nanotubes (SWNTs) or multi walled nanotubes (MWNTs) [6]. The type Iijima discovered CNTs in 1991 were MWNTs [9]. Within two years of Ijima's discovery, SWNTs were synthesized [10]. The difference between the two types of nanotube structure is the number of graphene sheets within the cylinder, with a SWNT containing only one sheet while MWNTs contain multiple sheets in a concentric arrangement of cylinders [6]. SWNTs have been found to be microporous while and MWNTs are mesoporous [11]. The lengths and diameters of these two types of CNT structures are also different, thus yielding different properties as well. For SWNTs,

the direction of the rolling of the graphite sheet is important as it determines whether the nanotube behaves as metallic or semiconducting [7].

The bond structure and physical structure of CNTs give them multifunctional and diverse properties (mechanical, electronic, thermal, and chemical). For SWNTs, a nanotube can be either of the armchair configuration or chiral depending on the appearance of a belt of carbon bonds around the diameter [1]. The high surface areas of CNTs give them the potential to be useful in many applications in which high surface area to volume ratio yields more optimal properties. These properties include high absorptivity, capacitance, and ability to diffuse charges [12].

2.1.2. Applications

Many potential applications for CNTs have been envisioned and applied to devices and products. The mechanical properties (e.g. specific stiffness, modulus over density, and Young's modulus over resistivity) of CNTs when normalized to density make them attractive for aerospace applications, especially when combined with polymers to create lightweight nanocomposites [13]. Furthermore, manipulation of CNT forests via mechanical densification has been shown to enhance these properties and create stronger CNT carpets with more structural support and protection [13].

One important application of CNTs are as electrodes for electrochemical systems in various devices and technologies ranging from storage and conversion devices to supercapacitors and batteries. The chemical stability of CNTs and other carbon materials in different temperatures as wells as their performance ability in a wide range of temperatures make them extremely attractive for electrochemical applications [2]. These applications include membranes for electrocatalytic reduction of oxygen, electrocatalytic oxidation of methanol, hydrogen

storage, lithium storage in lithium batters, and supercapacitors. Carbon materials are easily accessible, easily processed, and relatively low cost, which has generated great interest into research for using them as electrode materials in various systems that store energy, harvest mixing energy, or desalinate water [2, 14].

2.1.3. Methods of Characterization

Various characterization methods have been employed to study CNTs, with different methodologies yielding different information and benefits. The most widely used and power tool for characterization of CNTs is Raman spectroscopy. This method is non-destructive, fast, and does not require sample preparation. In combination with microscopy images, information on the diameter of SWNTs can be gathered [6]. Microscopy techniques, such as scanning tunneling microscopy (STM), transmission electron microscopy (TEM), scanning electron microscopy (SEM), and high-resolution electron microscopy (H-REM), are also used for nanotube characterization [6]. These images give the three-dimensional morphology of CNT nanotubes and yield the atomic structure and the electronic density of states (DOS). Imaging techniques can also be useful for studying the inter-shell spacing of MWNTs and expanded to studying the interlayer interactions within MWNTs [6]. Most often, however, only one of these imaging techniques is used for characterization.

The diameters of SWNTs can be studied in individual tubes by photoluminescence spectroscopy. The chemical structures can be studied through X-ray photoelectron spectroscopy (XPS), which can also be used to study MWNTs. Gas adsorption is usually used to determine the specific surface area of macroscopic samples of powders or porous materials, but can also be used for observing the layers within MWNTs [11]. Infrared spectroscopy is often used to

determine impurities in CNTs that are left over from synthesis or molecules capped on the nanotube surface [6]. To study larger scale structural details, X-ray diffraction or neutron diffraction is needed. Neutron diffraction is used to obtain details such has bond length, possible distortion, and the scattering vector. X-diffraction is a non-destructive method that is used to study the interlayer spacing, the structural strain, and the impurities of a CNT sample. Information on the diameters, the chirality distribution, and the alignment in CNTs can also be studied with X-ray diffraction data [9].

Numerical methods have been used to predict the interspacing of CNTs following mechanical densification [7]. However, these models have only been validated through SEM imaging, where CNT spacing has been estimated by measuring the distance between the brightest CNTs (representing the tubes in the top-most place) [7]. While these methods are shown to be accurate, the measurement is time-consuming and only allows for a representative sample measurement.

Although there are many methods that can be used to analyze the morphological, structural, and chemical characteristics of CNTs, many of the methods are either limiting in the information that can be obtained, require sample preparation, or destroy the CNT sample being studied. Furthermore, these methods are useful for characterizing individual nanotubes, but do not give information on CNT forest properties such as interspacing between CNTs. Thus, a method for direct characterization of CNT forests used in electrodes is needed.

2.2. Impedance of Porous Electrodes

Porous electrodes are used in a variety of systems such as fuel cells, dye sensitized solar cells, and energy storage and generation devices due to their high surface area to volume or weight ratio. It is important for electrode materials to have high surface areas because this allows for high capacitance [12], so porous materials are good candidates. The important parameters of characterization for porous materials are the length, diameter, the number of pores, the specific area, and the degree of uniformity of porous structure [8]. Porous electrodes in electrolyte solution can be represented in terms of circuit elements. Through the use electrochemical impedance spectroscopy, the physical parameters for porous electrodes can be modeled.

2.2.1. Electric Double Layer

In an electrochemical system in which an electrode is placed in an electrolyte solution, an electric double layer forms at the surface of an electrode when a potential is applied to a polarizable electrode [12]. Ions from the electrolyte are absorbed in the electrical double layer due to Coulombic interaction [15] and charge is accumulated in the double layer [2], as shown in Figure 2-1. The typical model of the electric double layer used to characterize materials with length scales larger than 2 nm is the Gouy-Chapman-Stern model, in which charges adhere close to the electrode surface in the Stern Layer and decreases exponentially with distance from the surface. The capacitance of electrodes can be studied by a variety of experimental methods, outlined, in section 3.2.3. Electrochemical Techniques.

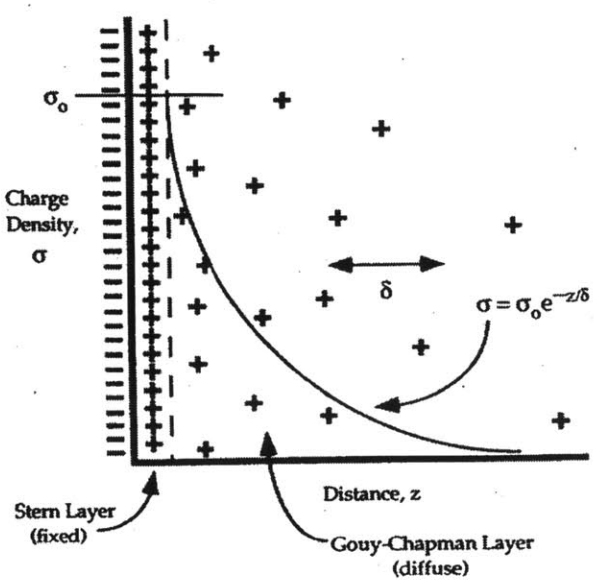

Figure 2-1. Schematic of the Electric Double Layer showing the Stern Layer where charges are accumulated and the Gouy-Chapman Layer where charge density σ decreases exponentially with distance from the surface. Figure from [17].

2.2.2. Electrochemical Impedance Spectroscopy

Impedance is the measured ability of a circuit to resist the flow of electrical current. It is measured by measuring the current I through an electrochemical cell when an AC potential E is applied. Impedance as a complex number is represented by,

$$Z(\omega) = \frac{E}{I} = Z_0 \exp(j\varphi) = Z_0(cos\varphi + jsin\varphi) \quad (1)$$

The expression for complex impedance Z(ω) comprises of a real and an imaginary part, which can be plotted into a Nyquist Plot, as shown in Figure 2-2, where the x-axis is the real part and the y-axis is the imaginary part. The impedance is represented as vector of length |Z| and the angle between the vector and the x-axis is the phase angle φ.

When *n* linear impedance elements are in series, the equivalent impedance is

$$Z_{eq} = Z_1 + Z_2 + \cdots + Z_n \quad (2)$$

For a parallel circuit, the equivalent impedance is represented as

$$\frac{1}{Z_{eq}} = \frac{1}{Z_1} + \frac{1}{Z_2} + \cdots + \frac{1}{Z_n} \tag{3}$$

When resistors are combined in series, both resistance and impedance goes up, while when capacitors are connected in series, capacitance goes down. Thus, impedance has an inverse relationship with capacitance in a circuit.

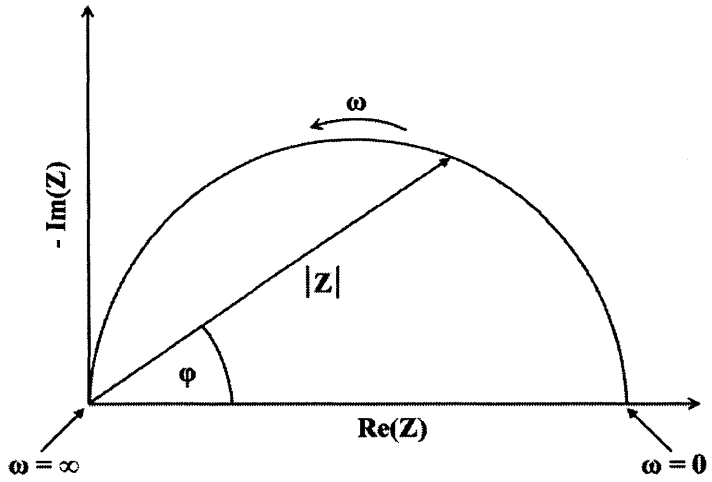

Figure 2-2. Nyquist plot for impedance data with the real component Re(Z) component on the x-axis and the imaginary component Im(Z) on the y-axis. |Z| is the vector representing the absolute impedance. Figure from [18].

2.2.3. Transmission Line Equivalent Circuit Model

Porous capacitive electrodes can be modeled using a transmission line equivalent model. The transmission line model of porous electrodes is used to describe the one dimensional, stepwise diffusion of ions within a pore of length *L*. Figure 2-3 shows a generic form of the transmission line model as a RC circuit representation and its impedance response. Suss *et al.* demonstrated the application of the transmission line model to hierarchical carbon aerogel electrodes with a bimodal pore size distribution [14].

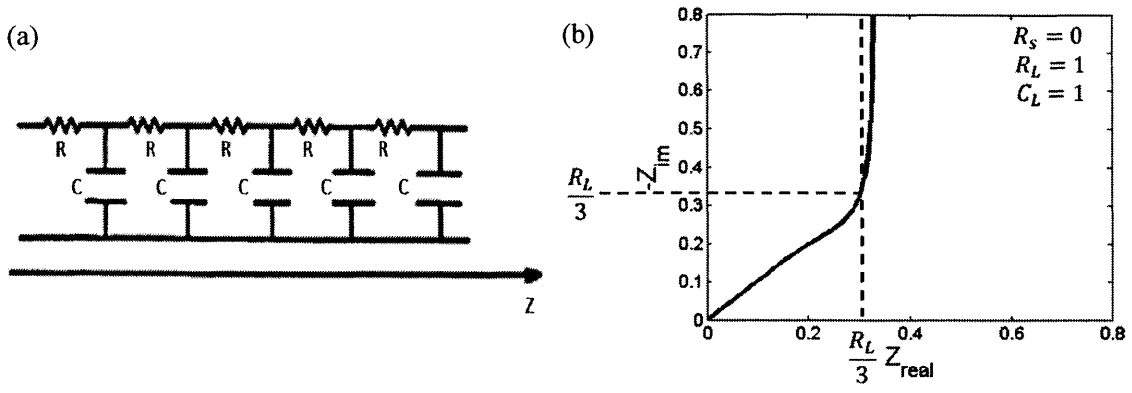

Figure 2-3. (a) RC circuit representation of the transmission line model and b) an impedance response of the transmission line model provided by H. Mutha.

2.3. Impedance Spectroscopy for Porosimetry Studies

Electrochemical techniques have been applied to characterize carbon electrodes in other studies and have been found to be a useful tool in the design and characterization of electrodes [2, 14, 16, 19]. Increased charge adsorption in electrodes is important for increased energy storage performance [12]. Furthermore, capacitance in porous electrodes has been found to generally scale with available surface area and the relative permittivity of the solution, and reciprocally dependent on the thickness of the double layer [2]. Techniques such as cyclic voltammetry, charge/discharge characteristics, and impedance spectroscopy used in evaluation of carbon materials as capacitors have been utilized [2].

Due to the high surface area nature of CNTs, CNTs have high potential for use in electrochemical systems. VA-CNTs have been shown to be efficient for charge accumulation as electrodes [2], making them a prospective candidate electrode material for electrochemical systems and impedance spectroscopy can be applied to model the porous nature of such base electrodes.

Song *et al.* demonstrated the use of electrochemical impedance data to relate to the geometric information of and to analyze the microstructures of various porous electrodes *in situ* [16]. In this work, this model is adapted to characterize the geometry of VA-CNT forests and to analyze the effect of increasing volume fraction of CNT carpets. For the VA-CNT electrodes, it is assumed that the spacing between CNTs are of cylindrical shape. It is also assumed that electrolyte conductivity and interfacial impedance are not a function of the location in a pore [16].

In accordance to Song *et al.*, the transmission line model (TLM) with pore size distributions (PSD) model can be formulated as

$$Z_{tot}(\omega: Y_P, \alpha_{\mu 0}, \sigma)^{-1} = Y_P \int_{-\infty}^{\infty} Z_p^*(\alpha)^{-1} k(y: 0,1) dy \quad (4),$$

in which $\alpha = \alpha(\omega, y: \alpha_{\mu 0}, \sigma)$, and $k(y: 0,1)$ is the normalized distribution model describing the variation in pore size. This equation contains the three parameters Y_p, α_μ, and σ that are used to fit the impedances of porous materials in Nyquist plots. Y_p is the parameter describing the total ionic conductance through pores and is represented by

$$Y_p = \frac{\kappa V_{tot}}{l_p^2} \quad (5),$$

where κ is the conductivity of the electrolyte, V_{tot} is the total porous electrode volume, and l_p is the pore length. The parameter α_μ is the representative penetrability coefficient for penetrability

$$\alpha = \left(\frac{1}{2l_p}\sqrt{\frac{\kappa r}{C_{dl}}}\right)\omega^{-0.5} \quad (6)$$

at a shift corresponding to distribution function k(x) with a mean μ and standardized deviation y $= (x - \mu)/\sigma$, thus yielding

$$\alpha_\mu = \left(\frac{1}{2l_p}\sqrt{\frac{\kappa r_\mu}{C_{dl}}}\right) \quad (7)$$

C_{dl} is the double layer capacitance and r_μ is the corresponding mode radius $r_\mu = r_o \exp(\mu)$, which is estimated as half the inter-CNT spacing for VA-CNTs, a value we hope to compare to solid-packing models for nanowire arrays [7]. The last parameter σ represents the distribution width of the distribution function $k(y)$.

Using these known relationships from the TSM-PSD model and the measureable characteristics, the three fitting parameters can be determined and fitted to impedance spectroscopy data, and the pore structures in the varying volume fraction carpets can be investigated.

Chapter 3. Experimental Methods

This research explores the possibility of using electrochemical impedance spectroscopy to characterize the porous structure in VA-CNT forests of varying volume fractions achieved via mechanical densification. The CNT samples acted as working electrodes in a three-probe electrode set-up placed in electrolyte solutions of 1 M and 0.5M sodium chloride (NaCl). The carbon nanotubes samples were placed in sample holders designed to ensure the most optimized one directional flow of ions. Step potentials from 0 V to 0.5 V, cyclic voltammetry from -0.5 V to 0.5 V, and impedance spectroscopy from 0 V to 0.5 V in increments of 0.1 V were run to collect electrochemical data on carbon nanotube samples.

3.1. Carbon Nanotube Sample Preparation

Samples of multi-walled CNT carpets of varying volume fractions were fabricated via chemical vapor deposition (CVD), characterized, and mechanically densified.

3.1.1. CVD Growth

VA-CNT forests were grown on pre-processed silicon wafers in a chemical vapor deposition (CVD) tube of 1 inch radius. Pre-prepared silicon wafers of 140 nm SiO_2 with a 20 nm alumina (Al_2O_3) coating and a 5 μm iron growth catalyst were cleaved using a diamond scribe into 1 cm by 1 cm squares. Four 1 cm by 1 cm pieces of silicon wafers were loaded into the 1-inch CVD tube furnace, growing four CNT carpets in each batch. CNTs are grown via the flow of helium, hydrogen, and ethylene gases for 7.5 minutes. The procedure includes a delamination step, etching away amorphous carbon at the catalyst site, weakening the bond between the forest and

the wafer, allowing for easier removal of the carpet. A detailed account of the recipe for CNT growth can be found in Appendix A.

3.1.2. Morphology Characterization

Height and mass measurements of CNT carpets needed to be obtained for use during the data analysis part. After the CNT-grown wafers were removed from the tube furnace, height measurements of each sample are taken. The forest still attached to the wafer is placed under an optical microscope. The height of the CNT sample is determined by measuring the difference in height of the focal plane between the Si wafer and the top of the forest. First, the lens is focused on the edge of the silicon wafer. Then the sample is moved so that the center of the surface of the sample is imaged and the number of rotations it takes to focus on the CNT carpet surface is counted, which each rotation representing 180 μm of height change of the microscope platform. Next, the carbon nanotube carpet is delaminated from the silicon wafers by using a razor blade and lightly tapping under the bottom of the carpets until the carpet is off the wafer. Once delaminated, CNT samples that were densified undergo the densification process described in 3.1.3. Afterwards, the mass of each CNT sample was measured on an Ohaus Discovery balance.

3.1.3. Mechanical Densification

Mechanical densification of as-grown 1 cm by 1 cm CNT carpets with 1% volume fraction was done to produce samples with variable targeted volume fractions of 2%, 5%, and 10%. As-grown CNT carpets are placed in a Teflon® densification platform of 1 cm channel width and 1 mm height (Figure 3-1) and mechanically densified by applying force onto the carpet in a direction perpendicular to the carbon nanotube forest. 2% and 5% volume fraction CNT samples were densified using uniaxial force to obtain samples with targeted dimensions of 0.5 cm by 1 cm and

0.2 cm by 1 cm, respectively. 10% volume fraction samples were densified biaxially to obtain samples were targeted dimensions of 0.285 cm by 0.35 cm from the as-grown 1 cm by 1 cm CNT forests. Table 3.1 shows the varying volume fractions of CNT samples prepared.

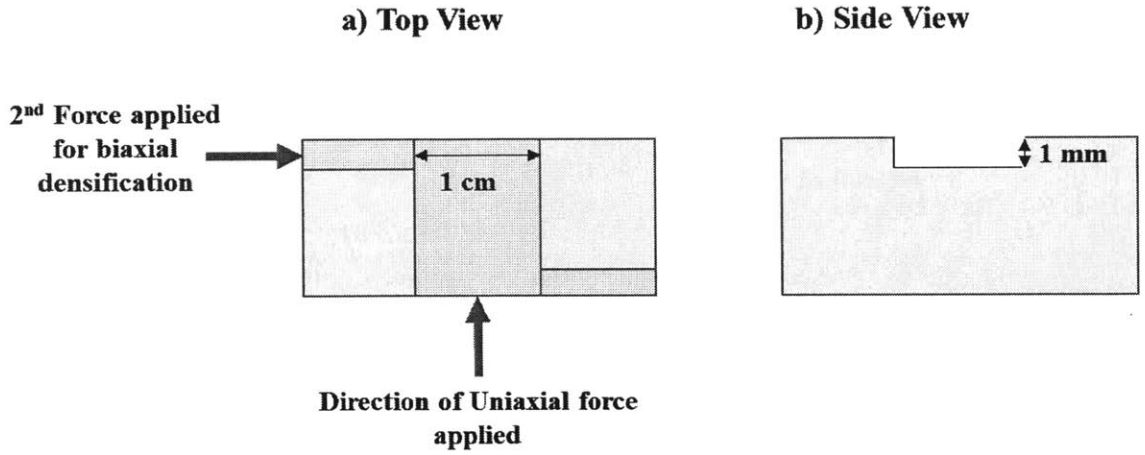

Figure 3-1. Schematic from (a) the top view and (b) the side view of the platform used for mechanical densification of CNT forests. Forests are placed in the 1 cm wide, 1 mm high channel and covered with a plastic piece to hold the forest down flat. A separate Teflon® piece is then used to apply a perpendicular compressive force along the channels in the directions indicated by the arrows onto the CNT forest to obtain the target dimensions.

Table 3-1. Targeted Volume Fractions and End Dimensions for Mechanical Densification

Targeted Volume Fraction	Targeted End Dimensions
1%	1 cm by 1 cm
2%	0.5 cm by 1 cm
5%	0.2 cm by 1 cm
10%	0.285 cm by 0.35 cm

3.2. Electrode Setup

To gather impedance spectra and other data needed for analysis, carbon nanotube carpets are placed as the working electrode in a three-electrode setup. The setup is connected to a Bio-Logic potentiostat and using EC-Lab® software, impedance spectroscopy, cyclic voltammetry, and step potential programs are ran.

3.2.1. Sample Holder Setup

The sample holder design is essential for ensuring that measurements of the working electrode isolate one dimensional porous diffusion into the VA-CNTs. Completely sealing the CNTs with only one plane exposed is key to conducting experiments that can be modeled with the appropriate boundary conditions.

In our design, a VA-CNT sample is placed near the end of a 1.5 cm by 3 cm platinum foil, with the base of the CNT carpet in direct contact with the surface of the foil. A piece of 86x86 PEEK (Polyetheretherketone) mesh with 0.0086-inch opening is placed over the sample and taped with a piece of 3M™ electromasking tape with a window approximately the length and width of the sample cut out, exposing the mesh covering the CNT carpet. The Pt foil with the CNT sample attached is then placed into a sample holder as shown in Figure 3-2. The sample holder is made of a 2 mm thick acrylic back, a 1/16 in thick GORE® GR compressible sheet gasket, and a 1.5 mm thick acrylic front piece stacked one on top of another and held together tightly by seven bolts and screws. The gasket and acrylic front contain windows of the dimensions in correspondence to the sample dimensions as shown in Table 3-2, with the acrylic window 81% smaller than the gasket window across all sample holders to ensure consistency in the interactive area of the CNT sample.

Afterwards, the lower two-thirds of the setup containing the sample window is dipped successively in 100% isopropanol (IPA), 75% isopropanol IPA 25% deionized water (DI water) solution, 50% IPA 50% DI water solution, 25% IPA 75% DI water solution, and 100% DI water for a few minutes in each. This method is used to replace the air in the CNT space with solution, and the slow replacement of IPA with DI water prevents bubbles from forming on the surface. This ensures complete wetting of the CNT sample.

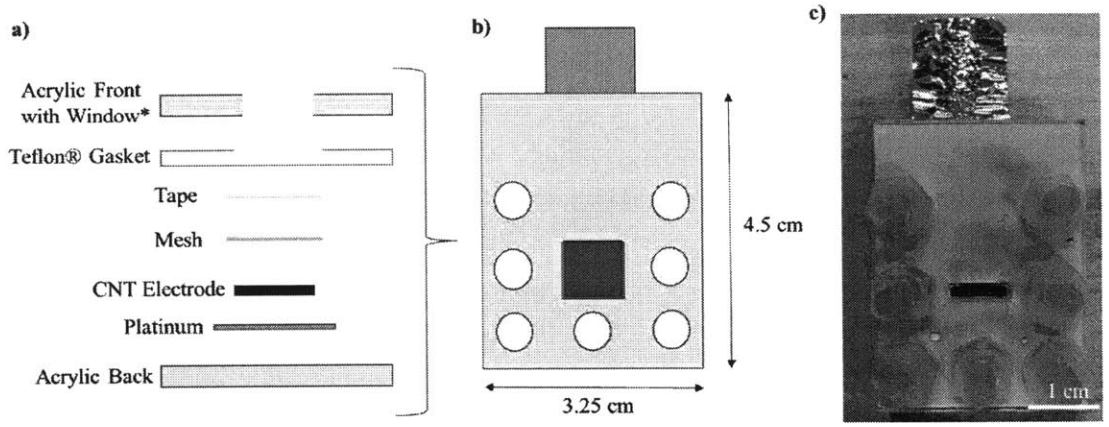

Figure 3-2. The working electrode setup holding the VA-CNT electrode shown as (a) the layers that are put together to create the holder, (b) a front view schematic of the sample holder for a 1% VA-CNT , and (c) an optical image of the front view of a sample holder for VA-CNT 5% volume fraction.

Table 3.2. Acrylic front and gasket window dimensions in sample holder setup.

CNT Volume Fraction	Dimensions of Acrylic Window	Dimensions of Gasket Window
1%	0.9 cm by 0.9 cm	1 cm by 1 cm
2%	0.45 cm by 0.9 cm	0.5 cm by 1 cm
5%	0.18 cm by 0.9 cm	0.2 cm by 1 cm
10%	0.2565 cm by 0.315 cm	0.285 cm by 0.35 cm

3.2.2. Three-Electrode Setup

A three-electrode setup with the sample as the working electrode, a 3 cm by 5 cm piece of platinum as the counter electrode, and a Beckman Coulter silver/silver chloride reference electrode is used to measure the electrochemical phenomena. Figure 3-3 depicts a diagram of a general three-electrode cell setup. The CNT sample is connected to the Bio-Logic potentiostat via the platinum piece that hangs outside the sample holder. The entire setup with all three electrodes is placed in a jar containing sodium chloride electrolyte solution. It is then left to sit in the NaCl solution for at least one hour to ensure that the forest is saturated in the solution. Programs containing the electrochemistry techniques, as described in 2.2.3., are run. Each sample is tested in both 1 M and 500 mM NaCl solutions in order to check that the impedance results only scale with solution conductivity and that no significant desalination is occurring in the solution.

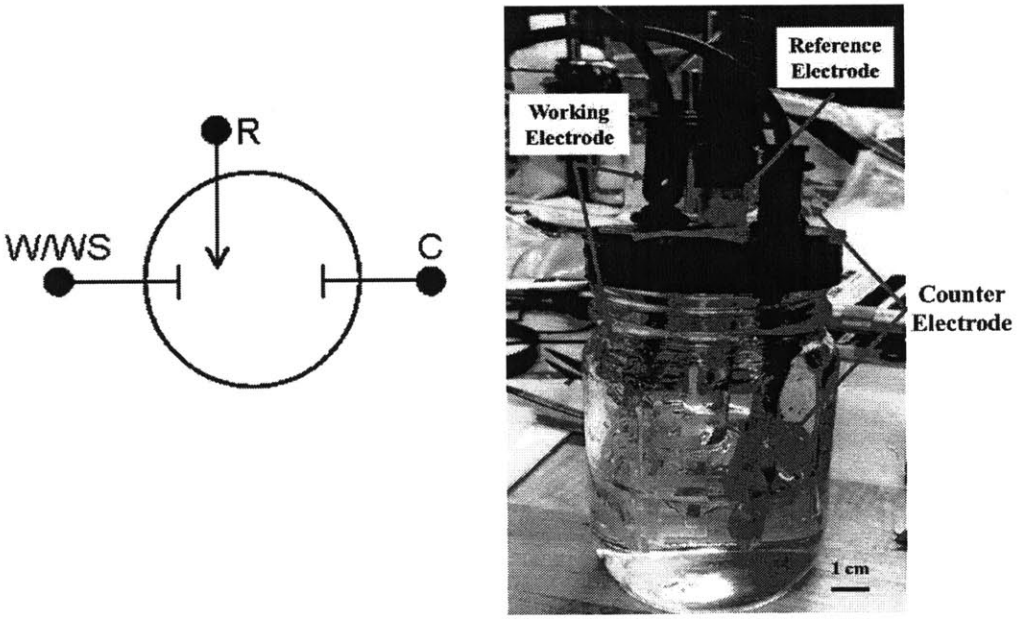

Figure 3-3. (a) A diagram and (b) an optical image of a three-electrode setup. The working electrode is indicated by W/WS, the reference electrode is indicated by R, and the counter electrode is indicated by C.

3.2.3. Electrochemical Techniques

The electrode setup is hooked up to Bio-Logic potentiostat instrument and connected to EC-Lab® V10.22. Appendix B details the settings and steps in the programs.

First, a step potential program containing a potentiostatic technique ramping the voltage in 0.1 V steps from 0 V to 0.5 V for five cycles is ran. The potentiontatic testing allows for calculation of the capacitance of the sample when plotting the charge response against the voltage applied, as per the equation

$$C = \frac{1}{V}\int I\,dt \tag{8}.$$

Next, a program containing cyclic voltammetry (CV) scans with an operating window of -0.5 V to 0.5 V and potentiostatic electrochemical impedance spectroscopy (PEIS) techniques in increments of 0.1 V from 0 V to 0.5 V is ran. The final operating conditions used for the CV scans and PEIS techniques were determined after iterations of testing different setup designs and other factors, as discussed in Section 4 on the optimization of the experimental methods.

CV scans were important for assuring that the electrode behavior is purely capacitive and the faradaic activity is minimized in the voltage window used. For CV scans, the more of a rectangular shape the scan is, the closer and electrode material is to ideal double layer capacitance behavior [2], as seen in Figure 3-4. Deviation from the rectangular shape exhibits pseudofaradaic reactions and possible redox reactions on the electrodes [2]. This is important in the data collection because by optimizing the behavior of the electrode, the more valid it is to say that the current is independent of potential and that there are no side reactions occurring on the electrodes. Details taken to determine the most optimal voltage window for running the CV scans will be discussed Section 4.

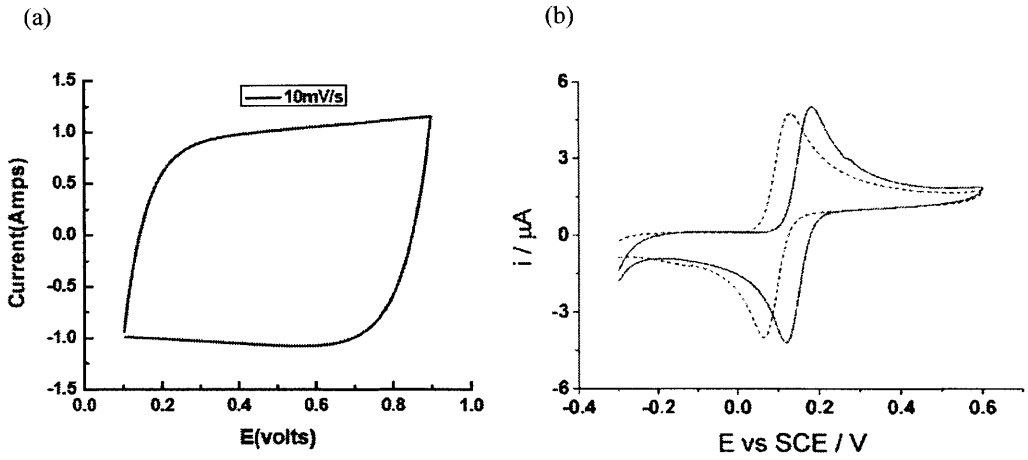

Figure 3-4. Cyclic voltammetry scan of (a) an ideal electrode with ideal double layer capacitor behavior [18] and (b) a faradaic electrode behavior [19].

Impedance spectroscopy results were run to study the porous electrode behavior as outlined in section 2.2.2. Electrochemical Impedance Spectroscopy. In addition, deviation from the expected one-dimensional diffusion model suggests the possible existence of sealing issues and possibly the existence of slow faradaic activity seen by the presence of a semi-circle, as indicated in Figure 3-5. For a porous electrode with no faradaic activity, the Nyquist plot should show a -45 degree phase angle at high frequency and then a vertical line at low frequency [8, 16] as shown in Figure 2-3 (b).

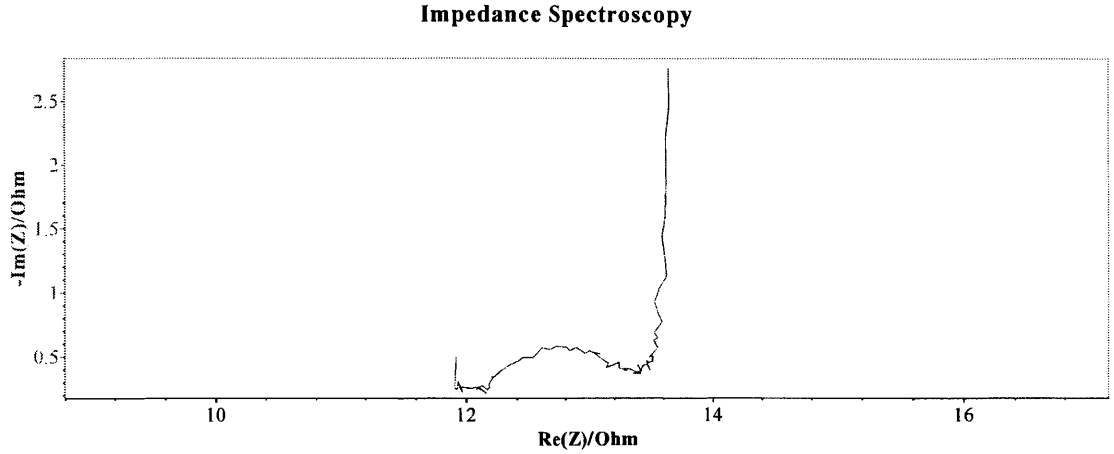

Figure 3-5. Example of impedance spectroscopy plot showing semicircular activity that implies contact resistance and deviation from ideal porous electrode behavior.

Chapter 4. Optimization of Experimental Methods

A significant amount of time and effort was put into the design of the experimental methods in order to create the most ideal conditions for gathering electrochemical data. Design changes in the sample holder, the electrode setup, and the program were done in attempt to achieve one-dimensional ion diffusion and to minimize the factors that can affect the data collected. The impacts of the changes were verified by looking at data collected through CV scans and PEIS plots. The following sub-sections will discuss the different components of the experimental method that were tested and altered to create an experiment that yields the most optimal data collection.

4.1. Sample Holder Setup and Configuration

The working electrode sample holder is one of the most important parts of the experiment that was optimized in terms of the materials used, the design and dimensions, and the layout of the components. The holder affected the interaction between the CNT sample electrode and the electrolyte, thus having a large effect on the data collection. It was important to have optimal sealing around the CNT carpet so that the ion transport was in one direction parallel to the pore length of the CNTs.

To ensure optimal data collection, the gasket material was a crucial component of the setup. Gaskets made of Teflon® and rubber were both tested, and it was determined that the Teflon® worked better to ensure that there was no leakage of water through the sides of the setup. The Nyquist impedance spectra from using the Teflon® gasket material had a high frequency slope that was closer to the ideal 45 degrees and the low frequency regions had a straighter slope, allowing the data to be fitted with the model. Figure 4-1 shows a comparison

between the Nyquist plots from using Teflon® gasket material versus rubber gasket material, and it is seen that the impedance spectra for Teflon® gasket material are closer together and do not deviate as much as the impedance spectra for rubber gasket material do when the voltage changes.

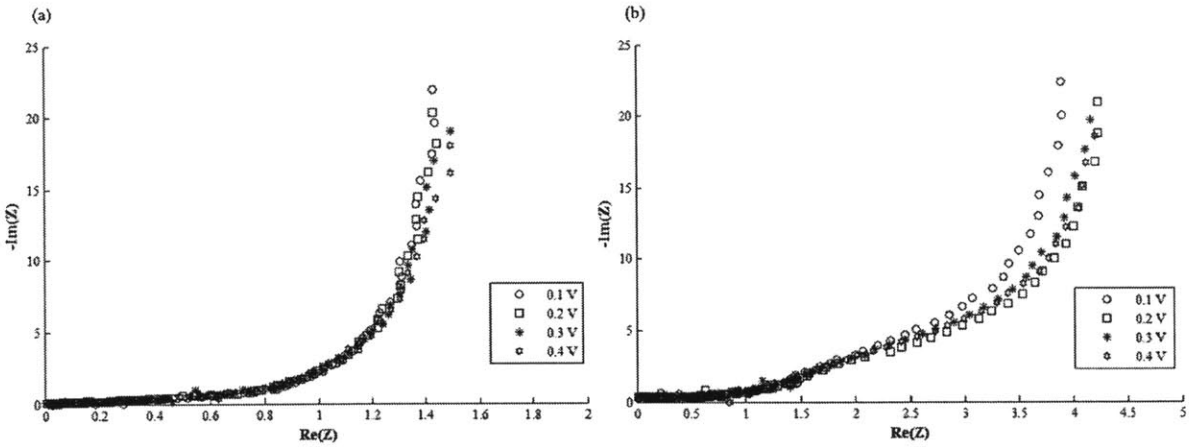

Figure 4-1. Comparison of Nyquist plots for sample holder using (a) Teflon® gasket material versus (b) rubber gasket material using a 1% VA-CNT electrode ran in 1 M NaCl. The Teflon® gasket material is shown to have better sealing and results in more ideal porous electrode behavior than the rubber gasket material.

Another reason why the design of the CNT electrode holder was important is because it is important to minimize the amount of resistance between the CNT forest electrode and the metal (the base electrode) in order to optimize the amount of charge transfer. Resistance and poor contact results in unreliable and inconsistent data that cannot be fitted with the model developed by Song *et al.* Two types of typical base electrode materials were tested: Ti foil and Pt foil. Pt foil yielded impedance spectra that demonstrated the porous electrode behavior of the VA-CNT forest and that can be fitted with the model. Even thinner Ti foil (25 μm) yielded semicircular impedance spectra (Pt foil was 50 μm). A comparison between the two metals as base electrodes is shown in Figure 4-2. Additionally, the effect of sputtering the CNT carpet's base with Ti was

considered and was realized that impedance data collected from samples that were unsputtered were closer to the ideal impedance plot, most likely due to less contact resistance without an extra material between the VA-CNT electrode and the base electrode.

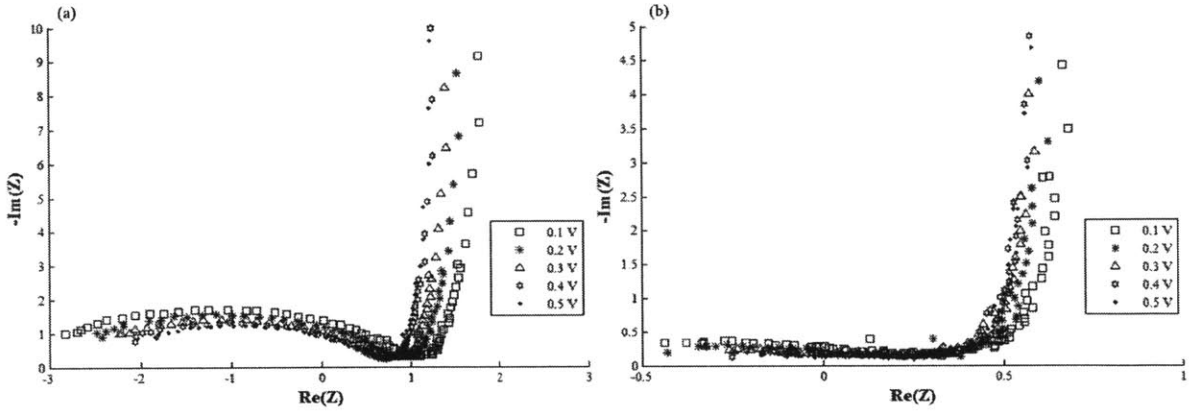

Figure 4-2. Comparison of Nyquist plots for sample holder using (a) Ti as the base electrode metal and (b) using a 1% VA-CNT electrode ran in 1 M NaCl. The Teflon® gasket material is shown to have better sealing and results in more ideal porous electrode behavior than rubber gasket material.

The setup was also tested with and without the use of tape over the mesh to hold down the CNT carpets, as shown in Figure 4-3. It was found that the tape provided an extra barrier around the CNT carpet, preventing the flow of the ions through the edges of the carpet. The tape also yielded impedance spectra that was similar and did not shift across the different voltages. The mesh was added to the setup because the mesh held the CNT carpets flatter and thus in contact with the metal base electrode while at the same time allowed permeability of ions through the porous CNT carpet. The mesh position within the setup was also considered and it was shown that the mesh was most effective when placed in direct contact with the CNT carpet and taped down onto the metal along its perimeter.

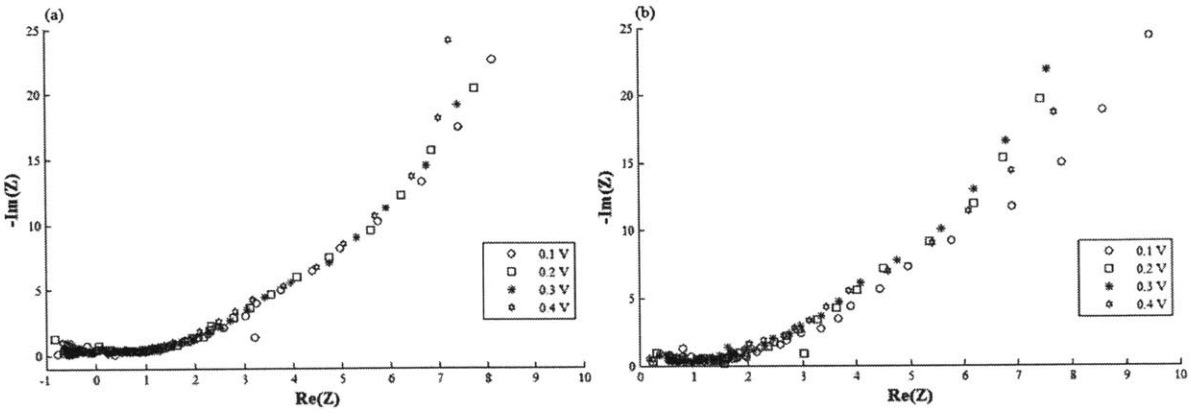

Figure 4-3. Comparison of Nyquist plots for sample holder (a) with tape versus (b) without tape using a 1% VA-CNT electrode ran in 1 M NaCl. The setup that used tape to hold down the mesh and the CNT electrode results in more impedance spectra that are consistent across voltages.

4.2. Electrode Setup and Procedure

The next part of the experimental setup that required attention to was the three-electrode setup used for running electrochemical techniques. The effect of moving the reference electrode in respect to the working electrode was experimented with and it was found that the distance between the reference and working electrodes did not affect the impedance spectra collected, as shown in Figure 4-4. In order to maintain consistency across the tests, the distances between the electrodes are keep constant and the working and counter electrodes are placed so that the CNT carpet faces parallel to the Pt counter electrode.

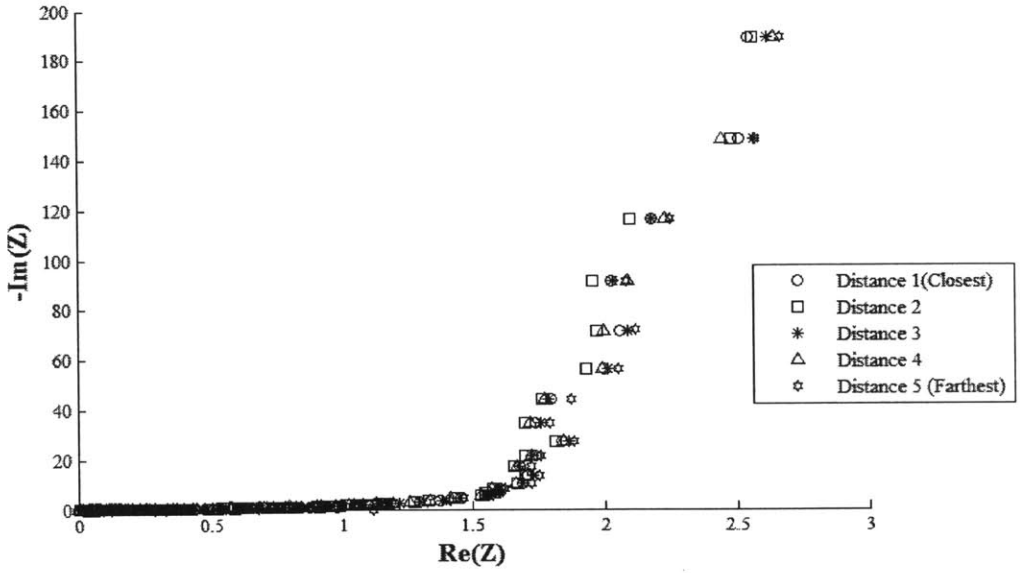

Figure 4-4. Impedance Spectra of a 2% VA-CNT electrode in 1 M NaCl placed in electrode setup in which distance between the reference and working electrodes are changed. It was seen that there was no significant change in the impedance spectra when the distance between the reference and working electrodes was increased from the closest possible to the furthest allowed by the electrode setup.

From the CV scans collected, it was seen that the duration in which the CNT carpet is saturated in the electrolyte solution affected the shape of the scans. The longer the carpet was soaked in the solution, the more wetted it was and the more rectangular the shape of the CV scans were. Furthermore, as the cycle number increased, the lines in the CV scan flattened and CV scan cycles that were closer to a rectangular shape. Thus, in order to make sure the CNT sample was closer to steady state when the impedance data is collected, samples setup in the electrode setup are left for at least an hour before the programs are ran.

4.3. Data Collection Program

The program details for running the electrochemical techniques were important in collecting the data as well because various factors, such as voltage window, scan rate, and time, all affected the quality of the data collected. To obtain Nyquist plots that can be modeled with the transmission line model, impedance at both high and low frequencies were need, thus resulting in the frequency range of 10 kHz to 10 mHz. Both positive and negative operating voltages were experimented with in the impedance spectroscopy scans. The resulting impedance graphs showed a deviation from ideal porous electrode capacitor behavior of a straight line in the low frequency region when the voltages ran were negative, as shown in the impedance spectra in Figure 4-5 with an operating voltage window of -0.2 V to 0.2 V. Thus, for the final program the voltage window used contained all positive voltages from 0 V to 0.5 V at 0.1 V intervals.

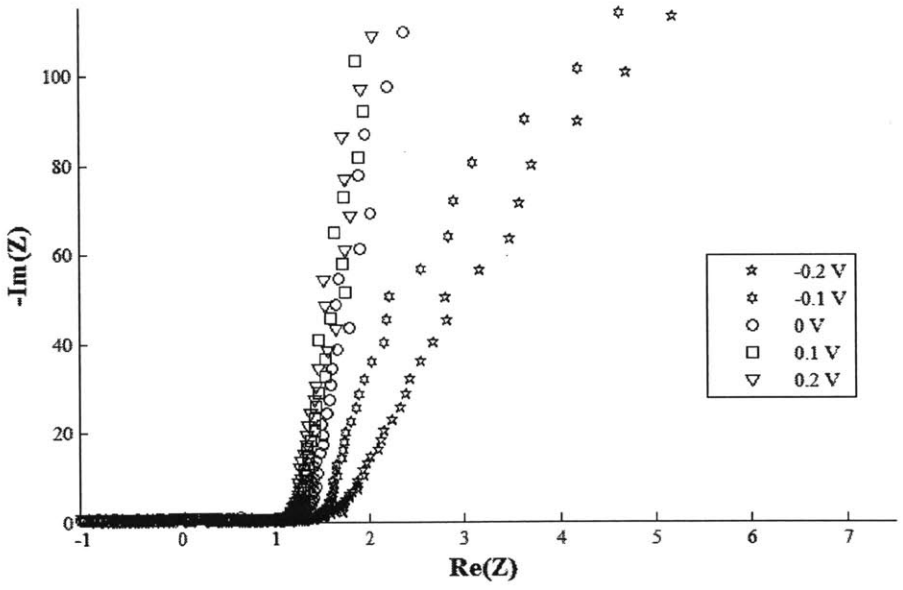

Figure 4-5. Impedance spectra for a 1% VA-CNT electrode operating with a -0.2 V to 0.2 V voltage window in 1 M NaCl solution. At low frequencies, the impedance spectra deviates from the straight slope expected of porous electrodes and starts becoming semicircular.

After iterations of tests and changes, the sample holder setup, electrode setup, and electrochemical program techniques are now optimal for gathering impedance data and data from other electrochemical techniques that are useful in the characterization of the porous electrode geometry. The final design of the sample holder, as shown in Figure 3-2A, contains Teflon® gasket and Pt base metal that uses tape to hold the VA-CNT electrode to the base electrode, which are design components that yielded the best results. The three-electrode cell setup is sufficient for gathering electrochemical data and the settings for the operation of the electrochemical techniques was found to be best at positive voltage windows. The optimization of the experimental setup is a crucial part of this project, and was found to have a significant role in the success of the project.

Chapter 5. Data Analysis and Discussion

CNT samples of 1%, 2%, 5%, and 10% volume fractions were tested and electrochemical data (via cyclic voltammetry, impedance spectroscopy, and potentiostatic step techniques) were collected for each. The impedance spectroscopy data is fitted with Song *et al.*'s model described in section 2.3 to calculate the three parameters Y_p, α_μ, and σ. This chaper will discuss the electrochemical data collected and the trends seen in them as well as the porosimetry parameter values generated from the fitting the data with Song *et al.*'s model.

5.1. Cyclic Voltammetry (CV) Scans

CV scans recorded the current response of the VA-CNT forest electrode sample to the voltage window applied. They were used check the porous behavior of the porous electrodes, to ensure minimal faradaic reactions on the electrode, and to verify the saturated, steady state status of the VA-CNT electrode in the solution. CV scans can also be used to check the capacitance response of the sample and verify the capacitance with the step potential data discussed in the following section (5.2). A sample CV scan obtained is shown in Figure 5-1, which shows a CV scan with five cycles obtained for a 1% VA-CNT forest operating in 1 M NaCl solution.

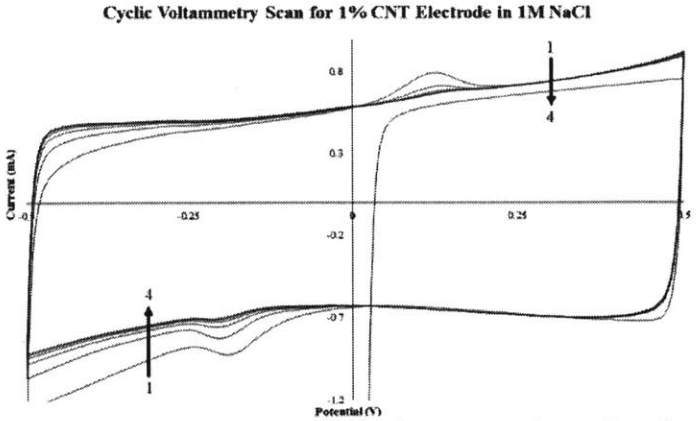

Figure 5-1. Sample CV scan (scan rate 10 mV/s) for a 1% volume fraction VA-CNT forest electrode in 1 M NaCl.

5.2. Potentiostatic Measurements

A series of constant potentials are applied to the setup and the current response with time is recorded using a step potential electrochemical spectroscopy technique is recorded. By integrating the current over time, the total charge can be plotted against the voltage and the capacitance of the CNT forest sample can be determined via equation 8. Figure 5-2 shows an example of a plot of the charge for a 1% VA-CNT electrode, where the slope of the plot is the capacitance. Typical sample capacitances ranged from 22.08 (SD 0.37) F/g to 44.97 (SD 0.92) F/g. To find the normalized C_{dl}, the capacitance of the sample is divided by the surface area of the CNTs calculated based on the sample mass and previous TEM information indicating a ~8 nm outer diameter CNT [7].

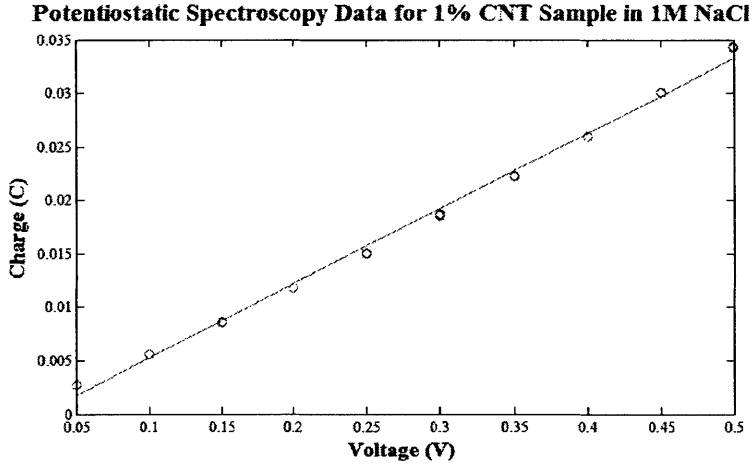

Figure 5-2. Sample potentiostatic spectroscopy data for a 1% VA-CNT forest tested in 1 M NaCl solution. The slope of a charge Q versus voltage V plot yields the capacitance of the electrode.

5.3. Impedance Spectroscopy Data

Impedance spectroscopy data was gathered for VA-CNT samples of targeted 1%, 2%, 5%, and 10% volume fractions, which are in Figure 5-3. As seen in the Nyquist plots in Figure 5-3 , the impedance spectra is independent of applied voltage in the tested window, indicating purely capacitive behavior. Even at different voltages, the impedance of the sample as shown in the

Nyquist plots should converge. The impedance data generally follows the shape of the ideal porous electrodes, with a shift in the low frequency regimes.

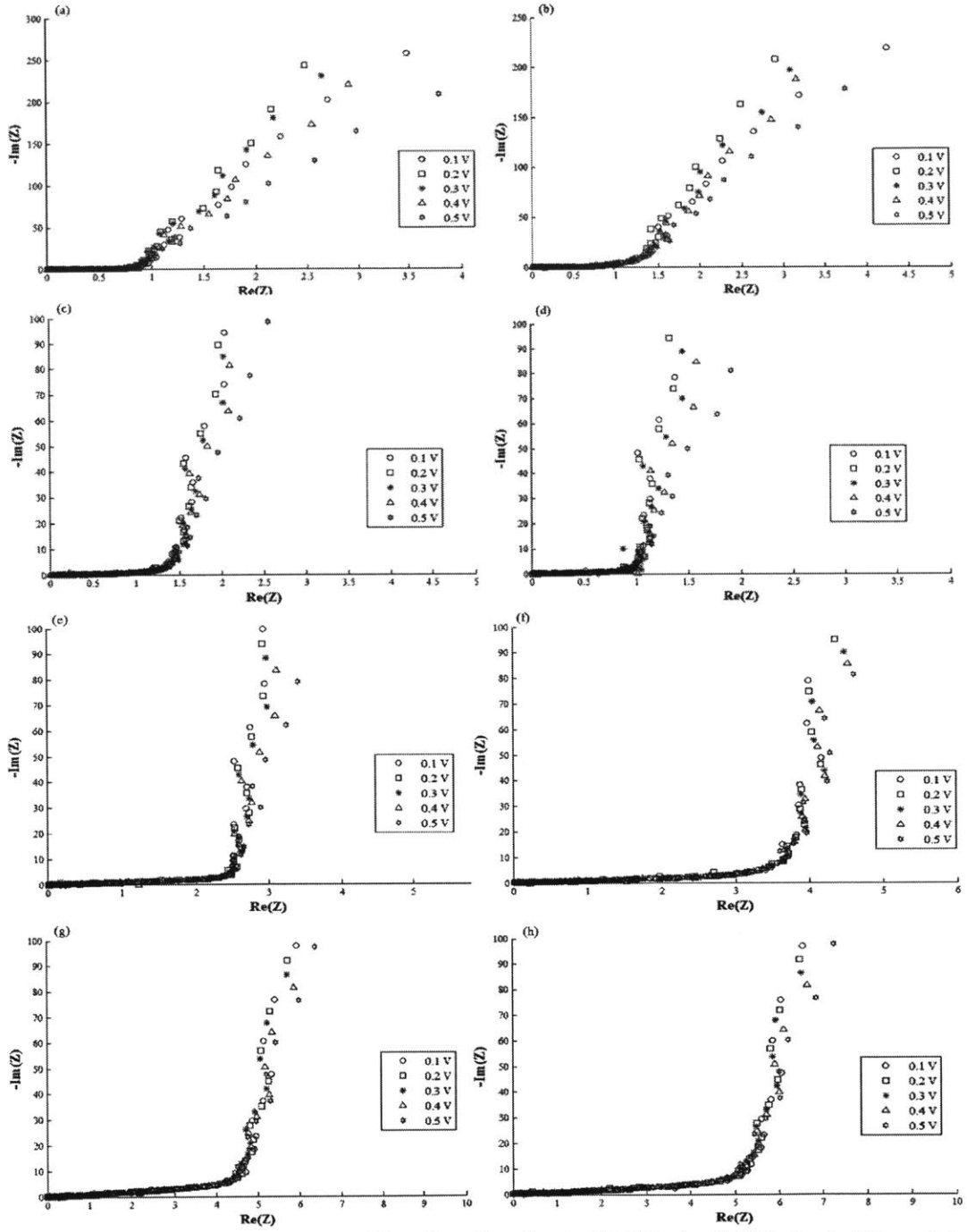

Figure 5-3. Impedance spectroscopy Nyquist plots for (a, b) 1%, (c, d) 2%, (e, f) 5%, and (g, h) 10% VA-CNT electrodes tested in 1 M NaCl. The impedance spectra across the operating voltages become increasingly precise as volume fraction increased.

The slope of the impedance data at high frequencies can be used to verify the porous electrode behavior by seeing if the slope is 45 degrees. This trend can be seen in Figure 5-4, which shows the average Nyquist plots zoomed into the high frequency regime for different volume fractions. As expected, the pore resistance increases with increasing volume fraction, shown by the length of the high frequency response (the region on the Nyquist plot given by the -45 degree slope. Figure 5-5 shows an overlay of the impedance spectra for the different volume fractions tested.

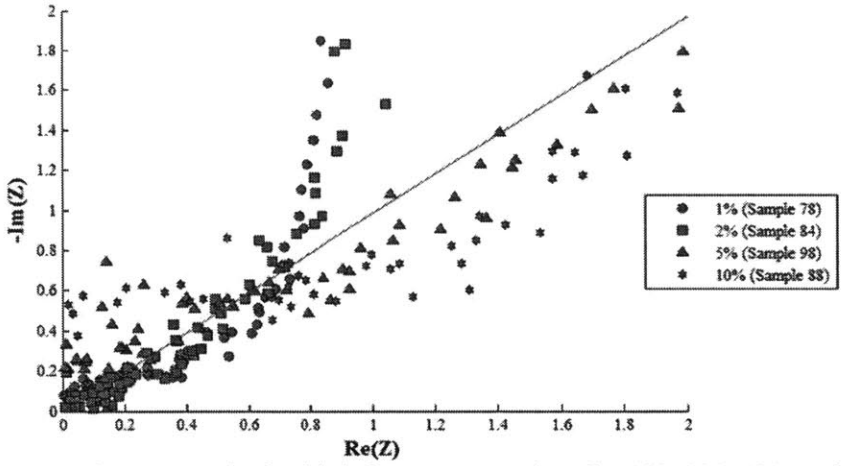

Figure 5-4. Impedance Data in the high frequency regime for 1%, 2%, 5%, and 10% CNT samples at 0.3 V in 1 M NaCl solution. The slopes of the impedance plot at high frequencies get closer to the ideal -45 degree slope (shown by straight line) as volume fraction increases.

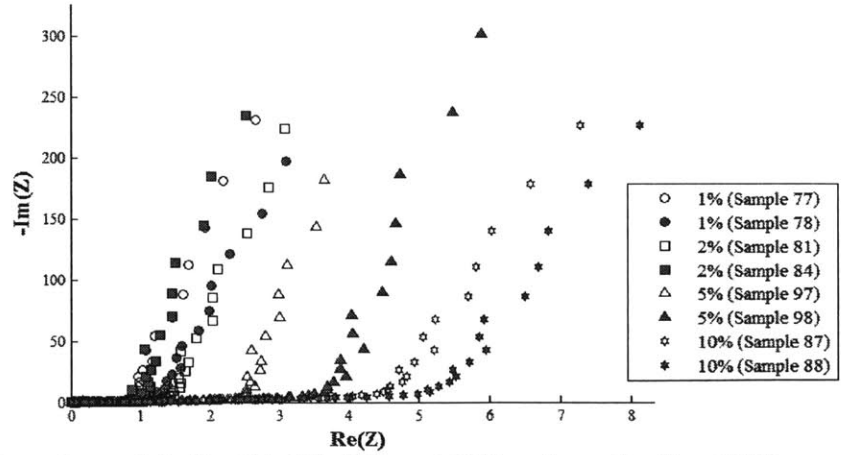

Figure 5-5. Impedance data for 1%, 2%, 5%, and 10% volume fraction CNT samples operating at 0.3 V and in 1 M NaCl. Overall impedance increases as the volume fraction increases.

Experiments were conducted in both 1 M and 500 mM NaCl to validate that no desalination is occuring and that the pores are saturated. We expect the impedance responses of a sample in either solution to be identical except for a factor of 2x the change related to solution conductivity. When testing in different concentrations of the electrolyte, it is expected that the overall impedance differs by the condutivity [3], as shown in the example in Figure 5-7. The overall impedance increased by twofold as the electroly solution concentration was halved. This trend was seen in all of the VA-CNT eelctrode samples and behaved as expected. The data colleted reflects anticipated behavior of the porous working electrode.

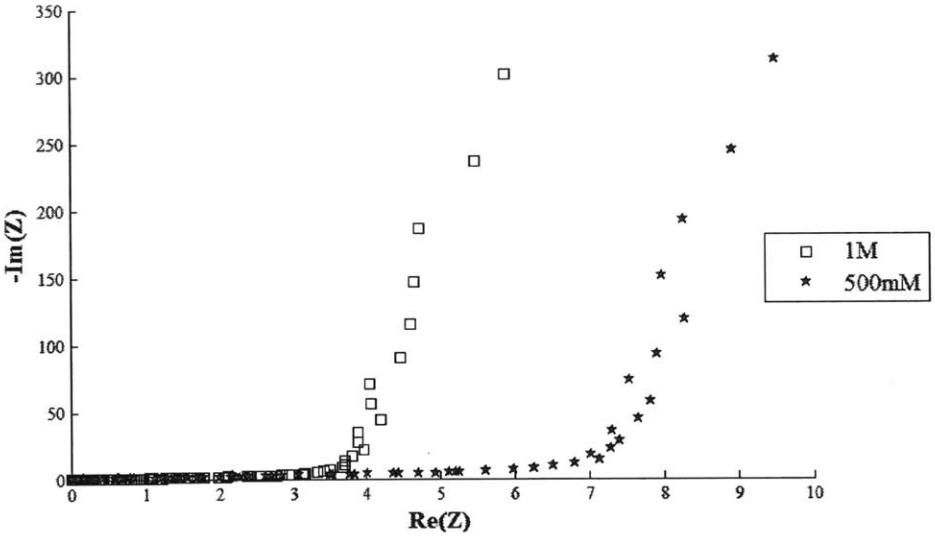

Figure 5-6. 500 mM NaCl electrolyte vs 1 M NaCl electrolyte 0.5 V impedance data for a 5% CNT sample, showing a difference in the overall impedance in different electrolyte concentrations.

Taking the Nyquist plots generated from the impedance data, the TSM-PSD model developed by Song *et al.* can be applied to fit the data collected. Figure 5-4 shows fits for a sample from each of the targeted volume fractions tested.

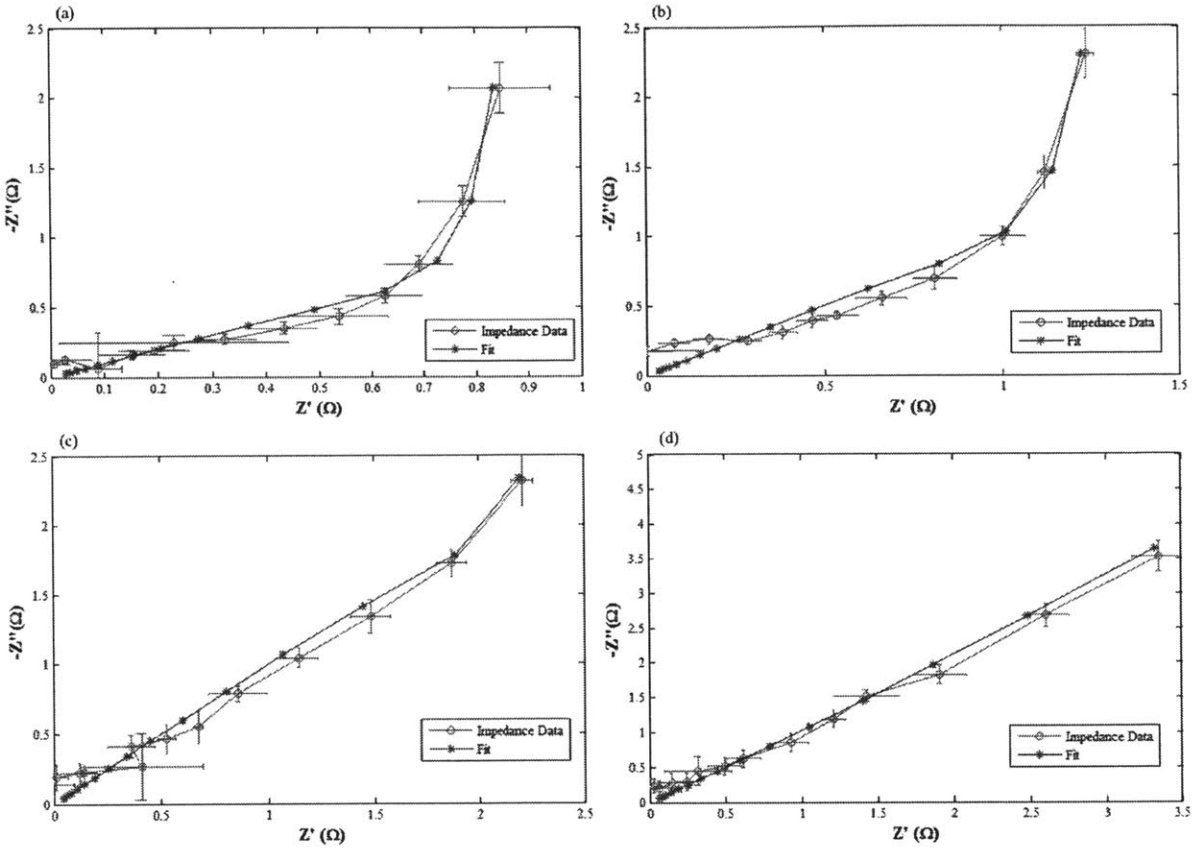

Figure 5-7. Examples of impedance data fitted with Song *et al.*'s model for (a) 1%, (b) 2%, (c) 5%, and (d) 10% VA-CNT electrodes in 1 M NaCl.

5.4. TLM-PSD Model Fit

5.4.1. Total Ionic Conductance Parameter Y_p

The experimental total ionic conductance parameter Y_p values were determined by fitting the TLM-PSD model to the impedance spectroscopy spectra collected for each sample. Figure 5-8 shows the Y_p values versus the volume fractions of CNT electrodes tested in 1 M and 500 mM NaCl solutions. The trend that is observed is a decay of Y_p as volume fraction increases, which matches with the expected behavior of Y_p because as volume fraction increases, the total porous volume V_{tot} decreases and Y_p is directly proportional to the porous volume. As vertically-aligned

CNTs are densified, the spacing between the pores decreases and ions have more difficulty reaching the electrode-electrolyte interface. In addition, since the spacing is decreased, ions have less mobility between the pores and thus increased ion resistance. The Y_p trends also follow as expected for different electrolyte solution concentration. The Y_p values for 500 mM are half of those for 1 M, which correlates with Equation 6 since the electrolyte conductivity is decreased in half.

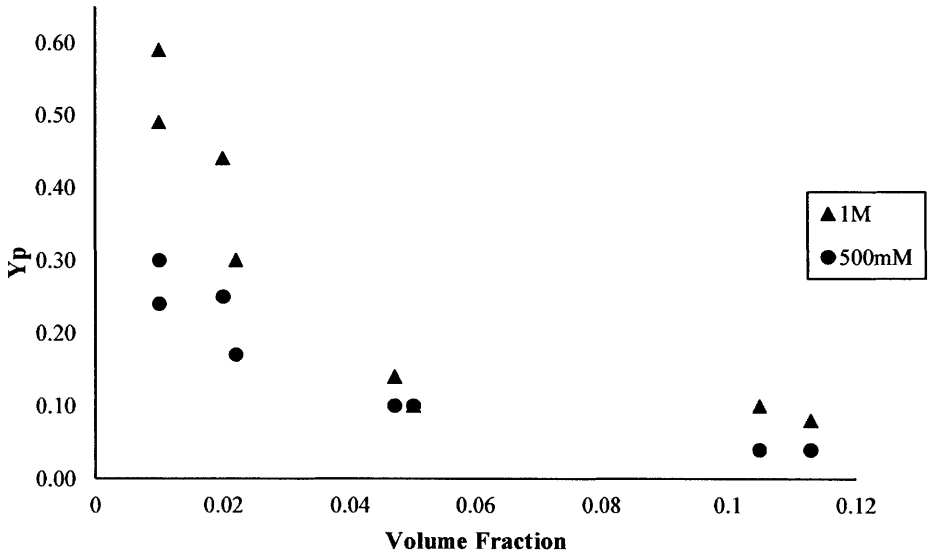

Figure 5-8. Experimental Y_p values determined via fitting for CNT samples of volume fractions tested in 1 M and 500 mM NaCl solutions.

Using the experimental Y_p extracted, the total porous electrode volume V_{tot} can be calculated using Equation (6). When normalized over the macroporous volume of the VA-CNT, its relationship relative to volume fraction V_f can be obtain and should follow $V_f = 1 - V_{tot}/V_{macro}$. Figure 5-9 shows that the ratios between the V_{tot} and the V_{macro} stay relatively consistent across the different volume fractions.

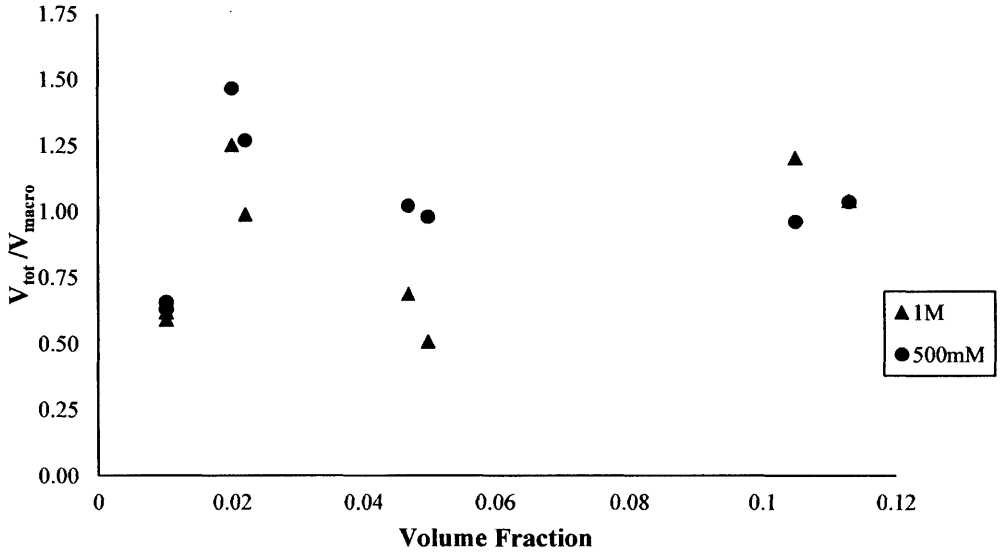

Figure 5-9. V_{tot}/V_{macro} ratios for CNT forests of the volume fractions tested in 1 M and 500 mM NaCl solutions.

Table 5-1 shows raw Y_p and V_{tot}/V_{macro} values corresponding to the exact volume fractions of each sample tested. Expected Y_p values were also calculated for each sample by using measurable values of CNT sample height, area, and mass, and can be found in Appendix C.

Table 5-1. Y_p and V_{tot}/V_{macro} ratios for CNT samples of 1%, 2%, 5%, and 10% targeted volume fractions tested in 1 M and 500 mM NaCl solutions.

Volume Fraction (Exact)	**1 M Y_p**	**1 M V_{tot}/V_{macro}**	**500 mM Y_p**	**500 mM V_{tot}/V_{macro}**
0.01	0.49	0.62	0.24	0.66
0.01	0.59	0.59	0.30	0.63
0.02	0.44	1.25	0.25	1.47
0.022	0.30	0.99	0.17	1.27
0.047	0.14	0.69	0.10	1.03
0.05	0.10	0.51	0.10	0.98
0.105	0.10	1.20	0.04	0.96
0.113	0.08	1.04	0.04	1.04

5.4.2. Mode penetrability coefficient α_μ

The mode penetrability coefficient α_μ is expected to decrease as volume fraction increases. As the spacing between CNT pores decreases, the penetration depth decreases. Even at the same frequency, the signal cannot travel as far into pores that are closer together than pores that are further apart from each other, yielding lower α_μ values. The actual mode penetrability coefficient α_μ values could be calculated using data collected from step potentials and the measurable values of VA-CNT forest height, area, and mass (Appendix C). The α_μ values ideally can also be determined by applying the TLM-PSD model developed by Song *et al.*, to the impedance spectroscopy data. However, this model did not yield anticipated α_μ values for some of the CNT samples the model was applied to. This suggests that there is a need for a model that fits better or that there are parameters that still need to be finalized and refined in the model developed by Song *et al.* The model used relied on various assumptions on the porous structure and ideal electrochemical behavior of porous electrodes that might not hold true for high density porous electrodes such as the VA-CNT forests with high volume fraction [16]. Improvements on the TLM-PSD model need to include more accurate input parameters that would fit for highly dense porous materials and need to incorporate more accurate assumptions of the physical characteristics of VA-CNT forests.

5.5. Sources of Error

The various problems that still exist with the analysis and application of the model to the impedance data collected indicates the possibility of various sources of error in the experiment. One source of error that is not accounted for in the modeling is the physical condition and stability of the VA-CNT forests. When CNTs face compressive, bending, or torsional stress, they

may buckle, which can occur during the mechanical densification of the VA-CNT forests described in section 3.1.3. Mechanical Densification. Signs of buckling exist in the form of metallic surfaces on the VA-CNT forests and samples that were used for data collection possibly contained buckled nanotubes. Another potential error during the mechanical densification is the change in height of the CNTs when placed in the densification setup. The densification setup is fabricated with a 1 mm height channel for the VA-CNT forests and many of the forests grown are taller than 1 mm. Thus, when the forest is mechanically densified, the cover piece of the densification setup holding the forest down may have caused potential bending of the nanotubes, which are assumed to be vertical in the model applied.

Other challenges that may cause error in the modeling is the translation of the mass of the VA-CNT sample to the number of CNTs present in the sample. When the mass is measured, as described in section 3.1.2. Morphology Characterization, the CNT carpet typically contain a layer of water absorbed to the surface of the CNTs. This layer over water will cause a higher mass to be measured than the actual mass of the carpet, which causes overprediction of the number of CNTs in the sample.

Chapter 6. Conclusions and Future Work

6.1. Conclusions

Effective *in situ* characterization methods of carbon nanotubes (CNT) are needed for geometric and performance characterization of CNT electrodes used in electrochemical systems. VA-CNT forest electrodes of densities from 1-10% were studied electrochemically in NaCl solutions to extrapolate information about the impedance response and geometry *in situ*. Expected trends in the CV scans and impedance spectra were obtained after careful debugging and optimization of various parameters in the experimental setup design and data collection procedure. Operational settings, such as the voltage window, electrochemical techniques were also found to be important in the collection of data suitable for analysis and fitting using Song *et al.*'s model. Thus, the optimization of various components of the experimental method yielded effective data collection.

Data collected from the electrochemical techniques aligned with the trends expected in the impedance response and the porous volumes. The CV scans and impedance spectra showed the porous behavior of the CNT electrodes. The impedance spectra showed that the volume fraction did not affect the shape of the impedance spectra, but affected the overall impedance. Data collected in 1 M NaCl and 500 mM NaCl showed the expected proportionality of the impedance to the conductivity of the solution as well as the consistency in the calculation parameters describing the geometric characteristics of the VA-CNT electrodes. The porous volume V_{tot} predicted by applying Song *et al.*'s model to the data collected follows the trend expected, in which increasing volume fraction yields lower ionic conductance Y_p and porous volume V_{tot}. Although the results support many of the expectations and assumptions made to apply the model used to characterize the VA-CNT porous geometry and structure, a more

detailed extension of Song *et al.*'s model is needed to fully characterize VA-CNT forests. This study has refined an experimental platform and collected extensive data for densified VA-CNT forests to further develop porosimetry models to extrapolate these values.

6.2. Future Work

The work done thus far provides the foundation for more research into *in situ* characterization of VA-CNT electrodes using electrochemical impedance spectroscopy measurements. In order to more accurately describe the porous structure and geometry of VA-CNT forests, more data collection needs to be done to refine the model. VA-CNT forests provide a unique advantage over the study of other porous materials: varying the pore length and exposed surface area can be done by simply varying growth time and wafer area during the growth process. We plan to investigate varying heights and total surface are to refine the model.

In addition, it would be exciting to push the data analysis to higher volume fractions to determine the limitations on both this experimental method as well as the limitations of mechanical densification of increased packing density. In addition, this data would allow us to refine the model, yield more accurate Y_p and α_μ values, and develop an understanding of the effect of high volume fractions. A better model would also provide further validation of results obtained so far and whether or not *Song et al.*'s model is applicable to VA-CNTs.

By applying impedance spectroscopy to model the porous characteristics of VA-CNT carpet, we hope this will become a practical and adequate method of obtaining information on CNTs while using them. Furthermore, we hope that this can become a widespread method that can be used in future studies on CNT electrodes and potentially other porous electrodes, allowing for a step closer towards new and powerful applications of CNTs in electrochemical systems.

Appendices

Appendix A. CNT Growth Recipe

VA-CNTs were grown via CVT on silicon wafers with 140 nm SiO_2 thickness that were cleaned using 3:1 Piranha acid, rinsed with DI water, and spun dry before they were prepared with electro-beam deposition, deposited with Al_2O_3 and iron. The 20 nm Al_2O_3 served as the diffusion barrier and the 5 nm iron acted as the growth catalyst. The program used to operate the controls for growing CNT in the tube furnace is as follows:

1. Cleaning the tube:
    - 1.1. Set helium to 1000 sccm and turn helium on.
    - 1.2. Wait for 4 min.
    - 1.3. Set hydrogen to 200 sccm and turn hydrogen on.
    - 1.4. Bubbler turned on at 0.7 bubble per second of water at ~600C (~0.01scfh).
    - 1.5. Set helium to 37 sccm.
    - 1.6. Set furnace 1 and furnace 2 to 200 degrees C.
    - 1.7. Turn furnace 1 and 2 on.
    - 1.8. Wait for 4.5 minutes.
    - 1.9. Wait until furnace 1 temperature is above 199 degrees C.
    - 1.10. Set furnace 1 to 740 degrees C and furnace 2 to 800 degrees C.
    - 1.11. Turn furnace 1 and furnace 2 on.
    - 1.12. Wait until furnace 1 temperature is above 738 degrees C.
    - 1.13. Wait for 5 min.
2. Growing CNTs:
    - 2.1. Set ethylene to 150 sccm and turn ethylene on.
    - 2.2. Wait for 7.5 minutes and turn ethylene off.
    - 2.3. Turn furnace 2 off.
3. Delamination Process:
    - 3.1. Set hydrogen to 250 sccm and wait 2 minutes.
    - 3.2. Wait 2 minutes.

3.3. Open furnace lids and turn off water.

3.4. Turn hydrogen and furnace 1 off.

3.5. Set helium to 920 sccm and wait 10 minutes.

3.6. Set helium to 100 sccm.

3.7. Wait until furnace 1 temperature is below 180 degrees C.

3.8. Turn helium off.

Appendix B. Electrochemical Technique Program Details

1. Potentiostatic Program

   The potentiostatic program comprised of two chronoamperometry programs that hold the potential at an voltage and then at 0 V, for a total of five loops times. Each loop is of an incremented voltage of 0.050 V between 0.050 V and 0.200 V. An example of the settings for a CA program used is as follows:

   E_i = 0.050 V vs. Ref; t_i = 2 min; dQ_M = 0.000 mA.h; dI = 5.000 μA; dQ = mA.h; dt = 0.100 s; dt_a = 0.10 s; E range min = -2.500 V; E range max = 2.500; Bandwidth = 7; Number of loops = 5

2. Impedance Spectroscopy + Cyclic Voltammetry

   The second set of programs ran consisted of potentio electrochemical impedance spectroscopy (PEIS) and cyclic voltammetry (CV) techniques. CA techniques were put into the program before the PEIS techniques hold the electrode at a constant voltage that is equivalent to the operating voltage of the PEIS technique to ensure steady state activity of the electrode. The operating voltages used for the CA and PEIS techniques in each round of data collection consisted of voltages from 0.000 V to 0.500 V at each 0.100 V. CV techniques were ran at the beginning and end of the entire set of CA and PEIS runs. The total run time for this program was 5 hours 14 minutes. Some of the other settings that are constant across all the programs are: Voltage Control Range: min = -10.00 V, max = 10.00 V; V, I filtering: 50 kHz; Channel: Grounded; Bandwidth = 7

   Examples of program settings used are shown below.

2.1. Cyclic Voltammetry

Ei = 0.000 V vs. Ref; dE/dt = 10.00 mV/s; E1 = 0.500 V vs. Ref; Step percent: 50; N = 10; E2 = -0.500 vs. Ref; nc cycles = 5; Ef = 0.000 V vs. Ref

2.2. Chronoamperometry / Chronocoulometry

E_i = 0.000 V vs. Ref; t_i = 5 min.; dI = 5.000 μA; dt = 0.1000 s; dta = 0.10 s; E range min; 10.000 V; E range max = 10.000 V

2.3. Potentio Electrochemical Impedance Spectroscopy

E = 0.0000 V vs. Ref; tE = 10.00 s; record = 1; dI = 0.000 mA; dt = 1.000 s; f_i = 10.000 kHz; f_f = 1.000 Hz; Sel N_d = 1; N_d = 20; N_t = 50; V_a = 5.0 mV; p_w = 0.10; N_a = 5

Appendix C. VA-CNT Sample Morphology Measurements

Sample #	Volume Fraction	Mass (mg)	Height (um)	Final Planar Area (mm^2)	V_{macro} (m^3)	1 M Y_P	1 M V_{tot}/V_{macro}	500 mM Y_P	500 mM V_{tot}/V_{macro}
77	0.01	3.02	1250	104.85	1.311E-07	0.49	0.62	0.24	0.66
78	0.01	3.41	1220	106.8	1.303E-07	0.59	0.59	0.30	0.63
84	0.02	2.21	1230	44.1	4.851E-08	0.44	1.25	0.25	1.47
81	0.022	2.15	1100	41.9	5.153E-08	0.30	0.99	0.17	1.27
97	0.047	3.47	1210	20.29	3.380E-08	0.14	0.69	0.10	1.03
98	0.05	2.09	1160	17.41	3.240E-08	0.10	0.51	0.10	0.98
88	0.105	2.54	1000	9.77	9.770E-09	0.10	1.20	0.04	0.96
87	0.113	2.66	1040	8.36	9.728E-09	0.08	1.04	0.04	1.04

Bibliography

[1] Baughman, R. H., Zakhidov, A. a, & de Heer, W. a. (2002). Carbon nanotubes--the route toward applications. *Science (New York, N.Y.)*, *297*(5582), 787–92.

[2] Frackowiak, E., & Béguin, F. (2001). Carbon materials for the electrochemical storage of energy in capacitors. *Carbon*, *39*(6), 937–950.

[3] Porada, S., Zhao, R., Van Der Wal, a., Presser, V., & Biesheuvel, P. M. (2013). Review on the science and technology of water desalination by capacitive deionization. *Progress in Materials Science*, *58*(8), 1388–1442.

[4] Wardle, B. L., Saito, D. S., García, E. J., Hart, a J., de Villoria, R. G., & Verploegen, E. a. (2008). Fabrication and characterization of ultrahigh-volume- fraction aligned carbon nanotube-polymer composites. Advanced Materials (Deerfield Beach, Fla.), 20(14), 2707–14.

[5] Fagerlund, G. (1973). Determination of specific surface by the BET method. *Mat??riaux et Constructions*, *6*(3), 239–245.

[6] Belin, T., & Epron, F. (2005). Characterization methods of carbon nanotubes: a review. *Materials Science and Engineering: B*, *119*(2), 105–118.

[7] Stein, I. Y., & Wardle, B. L. (2013). Coordination number model to quantify packing morphology of aligned nanowire arrays. *Physical Chemistry Chemical Physics : PCCP*, *15*(11), 4033–40.

[8] Gassa, L. M., Vilche, J. R., Ebert, M., Jüttner, K., & Lorenz, W. J. (1990). Electrochemical impedance spectroscopy on porous electrodes. *Journal of Applied Electrochemistry*, *20*(4), 677–685.

[9] S. Iijima, Nature 354 (1991) 56.

[10] Loiseau, A., Launois, P., Petit, P., Roche, S., & Salvetat, J.-P. (2006). Understanding Carbon Nanotubes. Springer-Verlag Berlin Heidelberg, 2006.

[11] Peigney, a., Laurent, C., Flahaut, E., Bacsa, R. R., & Rousset, a. (2001). Specific surface area of carbon nanotubes and bundles of carbon nanotubes. *Carbon*, *39*(4), 507–514.

[12] Lim, J.-A., Park, N.-S., Park, J.-S., & Choi, J.-H. (2009). Fabrication and characterization of a porous carbon electrode for desalination of brackish water. *Desalination*, *238*(1-3), 37–42.

[13] Garcia, E. J., Saito, D. S., Megalini, L., Hart, A. J., Villoria, R. G. De, & Wardle, B. L. (2009). Fabrication and Multifunctional Properties of High Volume Fraction Aligned Carbon Nanotube Thermoset Composites, *1*(1), 1–11.

[14] Suss, M. E., Baumann, T. F., Worsley, M. a., Rose, K. a., Jaramillo, T. F., Stadermann, M., & Santiago, J. G. (2013). Impedance-based study of capacitive porous carbon electrodes with hierarchical and bimodal porosity. *Journal of Power Sources*, *241*, 266–273.

[15] Oh, H. J., Lee, J. H., Ahn, H. J., Jeong, Y., Kim, Y. J., & Chi, C. S. (2006). Nanoporous activated carbon cloth for capacitive deionization of aqueous solution. *Thin Solid Films*, *515*(1), 220–225.

[16] Song, H.-K., Sung, J.-H., Jung, Y.-H., Lee, K.-H., Dao, L. H., Kim, M.-H., & Kim, H.-N. (2004). Electrochemical Porosimetry. *Journal of The Electrochemical Society*, *151*(3), E102.

[17] http://alcheme.tamu.edu/wp-content/uploads/2010/07/Picture36.png

[18] http://www.intechopen.com/source/html/16479/media/image56.png

[19] Varghese, O. K., Kichambre, P. D., Gong, D., Ong, K. G., Dickey, E. C., & Grimes, C. a. (2001). Gas sensing characteristics of multi-wall carbon nanotubes. *Sensors and Actuators B: Chemical*, *81*(1), 32–41.

[20] Hu, C. (2008). FLUID COKE DERIVED ACTIVATED CARBON AS ELECTRODE MATERIAL FOR ELECTROCHEMICAL Fluid coke Derived Activated Carbon as Electrode Material for Electrochemical Double Layer Capacitor. *Chemical Engineering*.

[21] Lee, P. T., Lowinsohn, D., & Compton, R. G. (2014). Glutathione in the Presence of Cysteine Using Catechol, 10395–10411.